nature communications

Article

https://doi.org/10.1038/s41467-026-69529-3

Climate extremes intensify global lake eutrophication by increasing the stress resistance of harmful bloom-forming algae

Received: 27 September 2025

Accepted: 3 February 2026

Published online: 17 February 2026

Check for updates

Chenyu Wang[1,4], Mengmeng Wang[1,4] ✉, Mengjiao Xie[1], Liya Qi[1], Menggaoshan Chen[1], Xiaohua Song[1], Zhi Zhou[2], Xiaoli Shi[3], Jingyun Yin[1], Yong'an Wei[1], Minxiang Xu[1], Liyu Pan[1], Ai-Jun Miao[1] ✉ & Liuyan Yang[1] ✉

Lake eutrophication is increasingly shaped by climate extremes, but how short-lived events yield persistent blooms remains unclear. Using global satellite records and laboratory and field experiments, here we show that heatwaves and extreme precipitation drive bloom dynamics beyond gradual warming. In harmful bloom-forming algae (HBFA), heatwaves trigger oxidative stress that rapidly induces intracellular polyphosphate and stabilisomes, dense polyphosphate-rich organelles. As intracellular ballast, stabilisomes drive downward migration, enabling access to sediment-derived phosphorus while avoiding thermal stress; CO_2 depletion elevates pH and reinforces a thermo-alkaline cascade amplification effect. Extreme precipitation delivers pulsed phosphorus inputs that are stored as intracellular polyphosphate, creating long-lived phosphorus reserves that prime later heatwaves. When precipitation pulses precede heatwaves, stabilisome formation, vertical migration, and bloom expansion are amplified, even in oligotrophic lakes. Compound climate extremes thus convert episodic disturbances into sustained ecological advantages, challenging nutrient-centric models and redefining bloom-risk prediction and management.

Eutrophication has become one of the most pervasive threats to freshwater ecosystems, driven historically by excessive nutrient loading and increasingly reshaped by a rapidly changing climate[1]. Although nutrient enrichment has long been viewed as the dominant force governing algal proliferation, global observations now reveal that climate-related disturbances, particularly short-lived but intense events such as heatwaves and extreme precipitation, recurrently disrupt lake biogeochemistry and trigger abrupt shifts in bloom trajectories. Heatwaves can accelerate algal metabolism[2], enhance nitrogen assimilation[3], and favor thermophilic and alkaline-tolerant taxa by intensifying CO_2 depletion and elevating water pH[4]. Extreme precipitation, in turn, delivers episodic pulses of nutrient-rich runoff that restructure lake trophic conditions over timescales of hours to days[5,6]. These climatic convulsions increasingly co-occur and appear to generate bloom trajectories that cannot be explained by gradual warming or nutrient inputs alone, suggesting the existence of rapid physiological responses that enable harmful bloom-forming algae (HBFA) to capitalize on environmental shocks.

Among the cellular strategies that may underlie this capacity, the intracellular accumulation of inorganic polyphosphate (polyP) has emerged as a candidate mechanism linking climatic perturbations to algal resilience. PolyP buffers oxidative stress, regulates energy

[1]Key Laboratory of Aquatic Ecosystem Health in the Middle and Lower Reaches of Yangtze River, State Key Laboratory of Water Pollution Control and Green Resource Recycling, School of Environment, Nanjing University, Nanjing, China. [2]School of Civil and Construction Engineering and Division of Environmental and Ecological Engineering, Purdue University, West Lafayette, IN, USA. [3]State Key Laboratory of Lake and Watershed Science for Water Security, Nanjing Institute of Geography and Limnology, Chinese Academy of Sciences, Nanjing, China. [4]These authors contributed equally: Chenyu Wang, Mengmeng Wang. ✉e-mail: wangmm@nju.edu.cn; miaoaj@nju.edu.cn; yangly@nju.edu.cn

balance, and mediates phosphorus storage under fluctuating environmental conditions[7,8]. It is sequestered within dense acidic organelles known as stabilisomes, which have been associated with cellular homeostasis and stress adaptation[9]. Yet despite their ubiquity across bloom-forming algae, the ecological significance of polyP and stabilisomes remains poorly resolved, particularly in the context of extreme climatic events. Whether heatwaves induce stabilisome formation that alters algal buoyancy and nutrient acquisition, and whether precipitation-driven phosphorus pulses generate a biochemical memory in phosphorus storage that primes HBFA for subsequent heat stress, are questions that remain unanswered. More broadly, it is unknown how the climate extremes interact with polyP-mediated processes to regulate bloom persistence across lakes of different trophic status.

These gaps highlight a fundamental challenge for contemporary eutrophication research: the mechanisms by which short-term climatic shocks are transformed into sustained ecological advantages for HBFA remain unresolved, limiting our ability to forecast bloom risk under future climate scenarios. Current conceptual frameworks predominantly emphasize nutrient supply or long-term warming and treat extreme events as transient disturbances. However, emerging evidence suggests that climate extremes may act as catalytic triggers that activate physiological pathways[4], potentially involving polyP accumulation and stabilisome formation, that restructure algal behavior, stress tolerance, and vertical mobility on timescales much longer than the disturbances themselves. A mechanistic, cross-scale understanding of these processes is urgently needed. Addressing these unresolved questions requires a framework that links short-term climatic shocks to the physiological pathways that sustain harmful algal persistence.

Here, we combine two decades of global satellite observations with controlled laboratory assays and field-derived incubations to quantify how heatwaves and extreme precipitation regulate polyP metabolism, stabilisome formation, and vertical migration in HBFA. We show that heatwaves induce oxidative stress that triggers rapid polyP accumulation and the formation of dense stabilisomes that function as intracellular ballast, enhancing downward migration, thermal avoidance, and access to sediment-derived phosphorus. We further demonstrate that precipitation-driven phosphorus pulses are rapidly assimilated and stored as polyP, creating a biochemical memory in phosphorus storage that primes HBFA for subsequent heatwaves. Together, these mechanisms reveal how compound climate extremes convert transient disturbances into sustained physiological and ecological advantages. These findings provide a mechanistic framework that reconciles global eutrophication trends with climate extremes and highlight the need to incorporate compound-event dynamics into bloom prediction and lake-management strategies.

Results and discussion

Climate extremes reshape the global trajectory of lake eutrophication

As shown in Fig. 1a, b, global lake algal bloom scale, indexed by global median bloom frequency, exhibited distinctly irregular fluctuations from 2003 to 2022 across more than 600 lakes worldwide with bloom occurrences persisting for over a decade. Despite this variability, its long-term increase aligns with the rising trajectories of major anthropogenic and climatic drivers, including population growth, surface warming, and intensifying precipitation (Fig. 1b). Although ~47% of global lake degradation has been attributed to intensified land use and nutrient emissions[10], such gradually increasing pressures alone cannot account for the pronounced interannual variability in algal bloom. Consistent with this discrepancy, previous machine-learning analyses identified temperature anomalies and extreme precipitation as the dominant predictors of future algal bloom trajectories[11], suggesting that short-lived climatic perturbations exert disproportionately strong influence. Extending these findings, our generalized additive model (GAM) analysis further shows that temperature anomalies and extreme precipitation metrics retain consistently high importance across alternative model formulations, whereas gradual climatic indicators exhibit greater sensitivity to model structure (Fig. 1c). Together with the documented rise in compound lake-extreme events[12], these findings indicate that episodic climatic disturbances rather than long-term mean conditions primarily govern the interannual variability and amplification of contemporary eutrophication.

Although climate extremes dominate sharp interannual fluctuations in global median bloom frequency, long-term demographic pressure and gradual climate change continue to shape the baseline trophic state of lakes. Model-based importance analysis indicate that human population, temperature, and precipitation remain non-negligible contributors to global chlorophyll-a (Chl-a) variability (Fig. 1c), supporting the role of long-term drivers in shaping the baseline eutrophication trajectory[13]. Consistent with this pattern, analyses of 547 globally distributed bloom-prone lakes showed that Chl-a increased with watershed population density and with aqueous total nitrogen (TN) and total phosphorus (TP) concentrations (Fig. S1a), reflecting the foundational role of nutrient enrichment in supporting algal blooms[14].

Chl-a concentrations are generally projected to rise under future climate scenarios, with nutrients acting as the dominant amplifiers in landscapes undergoing intensified land use[11]. Nevertheless, reductions in watershed nutrient inputs can suppress algal bloom, demonstrating that eutrophication remains responsive to nutrient management even under warming[15]. Yet this expectation does not always hold. In China, for example, harmful algal blooms have intensified despite declining external nutrient loads[16], suggesting that climatic disturbances may interact with large internal legacy nutrient pools to push systems across ecological thresholds[17]. The nonlinear relationships between Chl-a and either temperature or precipitation (Fig. S1a) further support this view, indicating that climatic forcing modulates bloom outcomes through its interactions with internal nutrient dynamics, and that the strength of these interactions varies across management regimes.

Although global human population and Chl-a exhibit broadly synchronous upward trends, multivariable importance analyses indicate that hydrometeorological extremes consistently rank among the most influential predictors of Chl-a variability once climate and anthropogenic drivers are considered together (Fig. 1c). Specifically, temperature anomalies and multiple indices of extreme precipitation consistently explain a larger share of Chl-a variability and retain stable importance across alternative model formulations, indicating that lake algal blooms are more sensitive to short-term climatic perturbations. These results support a coherent conclusion that, under contemporary climate conditions, hydrometeorological extremes exert a more direct and stronger control on bloom expansion than do gradual anthropogenic and climatic changes. Independent evidence corroborates this pattern: aquatic heatwaves alone can increase surface Chl-a by more than 20% and occur alongside bloom events at significantly above-random frequencies[18]. Event-attribution analyses further reveal that 24 of 29 documented summer lake heatwaves coincided with pronounced Chl-a increases, with mean enhancements exceeding 50% in low-nutrient lakes[19]. Together, these findings indicate that hydrometeorological extremes function as threshold-like disturbances that rapidly translate accumulated nutrient legacies into elevated algal biomass, generating eutrophication risks that exceed those imposed by gradual warming alone.

In addition to governing Chl-a variability, climate extremes also reshape nutrient availability, thereby influencing the resource environment that supports algal bloom development. To evaluate nutrient-response pathways, TN and TP dynamics were modeled across 547 lakes using GAMs (Fig. S1b). Strong positive associations with watershed population density reflected sustained anthropogenic nutrient

https://doi.org/10.1038/s41467-026-69529-3

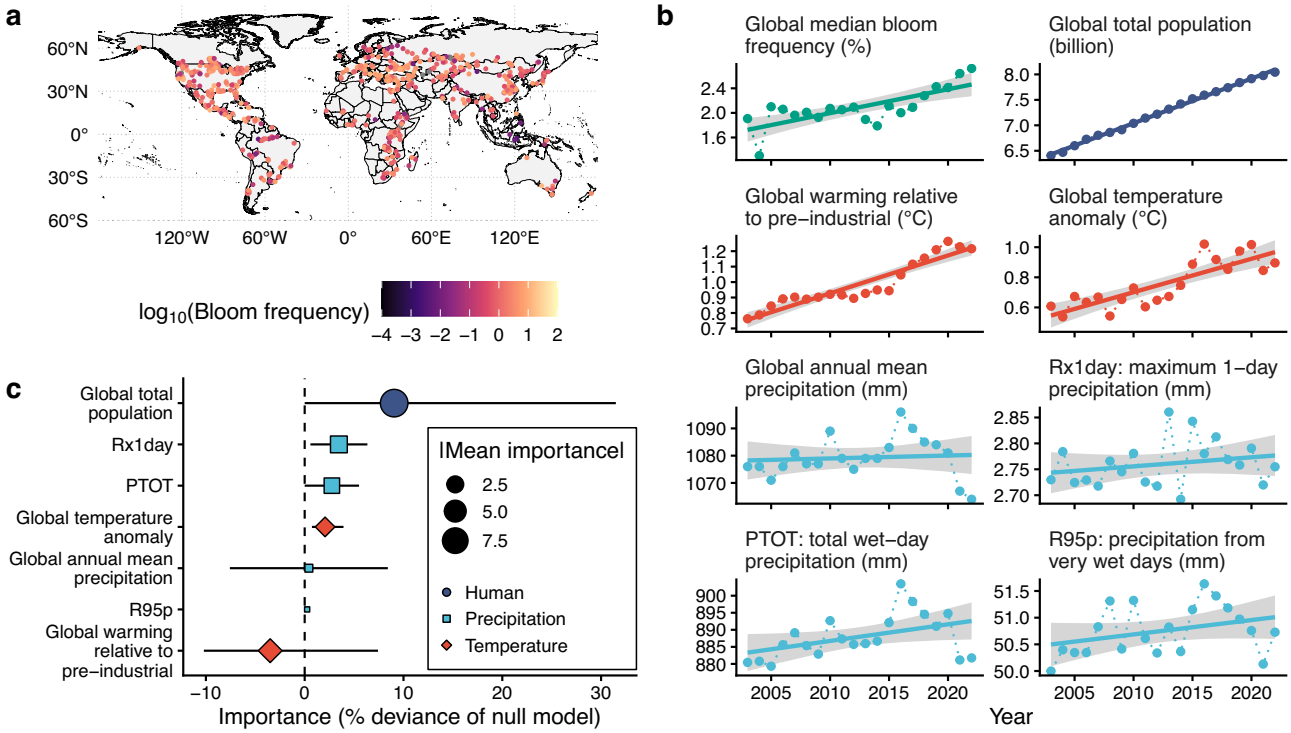

Fig. 1 | Global patterns of algal bloom frequency in large shallow lakes and their major drivers. a Spatial distribution of algal bloom frequency in 607 large shallow lakes worldwide that experienced blooms for more than 10 years during 2003–2022, shown for the year 2022. Colors indicate the logarithm of bloom frequency [$\log_{10}$ (bloom frequency)]. **b** Temporal trends (2003–2022) in global median bloom frequency (%) and major anthropogenic and climatic drivers, including global total population, global warming relative to pre-industrial levels, global temperature anomaly, the annual maximum 1-day precipitation amount (Rx1day), the cumulative precipitation associated with extreme events above the 95th percentile (PTOT), and the annual total precipitation from days exceeding the 95th percentile of the reference period (R95p). Solid lines represent linear fits, and shaded areas indicate 95% confidence intervals. **c** Variable-importance analysis based on generalized additive model (GAM), showing the relative contributions of anthropogenic pressure (population), temperature metrics, and precipitation and extreme-precipitation metrics to global median bloom frequency. Points denote mean importance across the candidate model set, horizontal bars indicate the minimum–maximum range, and point size scales with the absolute mean importance; the dashed vertical line marks zero contribution. Analyses were conducted using 607 large shallow lakes worldwide that experienced persistent blooms for >10 years during 2003–2022; The unit of study is the lake (lake-scale annual bloom frequency).

inputs, whereas nonlinear dependencies on temperature and precipitation revealed an additional climate-sensitive mechanism (Fig. S1b). Storm events can abruptly increase external loading through runoff and sediment resuspension, especially in shallow or disturbed catchments[20,21]. At event-dominated timescales, stormflow pipelines deliver high-flux, short-duration nutrient pulses to lake inlets, while sediment resuspension mobilizes benthic nutrient reserves into bioavailable forms, producing bloom peaks that frequently lag rainfall[18]. Thus, climate extremes can transiently elevate nutrient availability for HBFA through pulsed inputs even without changes in external anthropogenic loads.

It should be noted that the bloom-frequency metric used here is derived from surface-sensitive satellite observations and therefore primarily captures surface or near-surface algal accumulations, potentially underrepresenting subsurface biomass in some lake systems. Moreover, while the use of a single, internally consistent MODIS–Aqua sensor and a validated detection framework minimizes cross-sensor and classification uncertainties, lake-specific hydrodynamics and internal nutrient cycling processes are not explicitly resolved in this global-scale analysis.

Collectively, these results demonstrate that contemporary eutrophication risk is governed by the interaction between long-term nutrient enrichment and short-duration climate extremes. Rather than diminishing the importance of anthropogenic drivers, hydrometeorological extremes act as pulse-like amplifiers that rapidly convert pre-existing nutrient legacies into bloom expansion. This pulse-sensitive coupling between episodic climatic disturbances and accumulated nutrient reservoirs defines a central feature of modern lake eutrophication dynamics, underscoring the need to complement mean-load reduction strategies with management approaches that explicitly address climate extremes and nutrient pulse regimes. Recent evidence showing that nutrient-pulse regimes govern phytoplankton functional stability provides further mechanistic support for shifting from mean-load reduction to pulse-oriented management strategies[12,17,22]. The mechanistic pathways through which climate extremes intensify eutrophication, including their effects on nutrient pulses and HBFA stress physiology, are examined in the following sections.

Heatwaves promote bloom persistence by enhancing the stress resistance of HBFA

Heatwaves impose pronounced oxidative stress on HBFA while simultaneously triggering physiological priming that enhances their capacity for survival and regrowth. In our experiments, exposure to 40 °C increased reactive oxygen species (ROS; O_2^-, H_2O_2) by 35.9–215.8%, elevated antioxidant enzyme activities (superoxide dismutase [SOD] and catalase [CAT]) by 0.55–6.30 fold, and raised malondialdehyde (MDA) levels by ~0.81–1.96 fold relative to 25 °C (Fig. 2a). Photosynthetic performance declined in parallel, as indicated by reductions in effective quantum yield of PSII (Y[II]), maximum quantum yield of PSII (F_v/F_m), and maximum electron transport rate (ETR_m) (Fig. S2a). These responses mirror those observed in *Scenedesmus*

https://doi.org/10.1038/s41467-026-69529-3

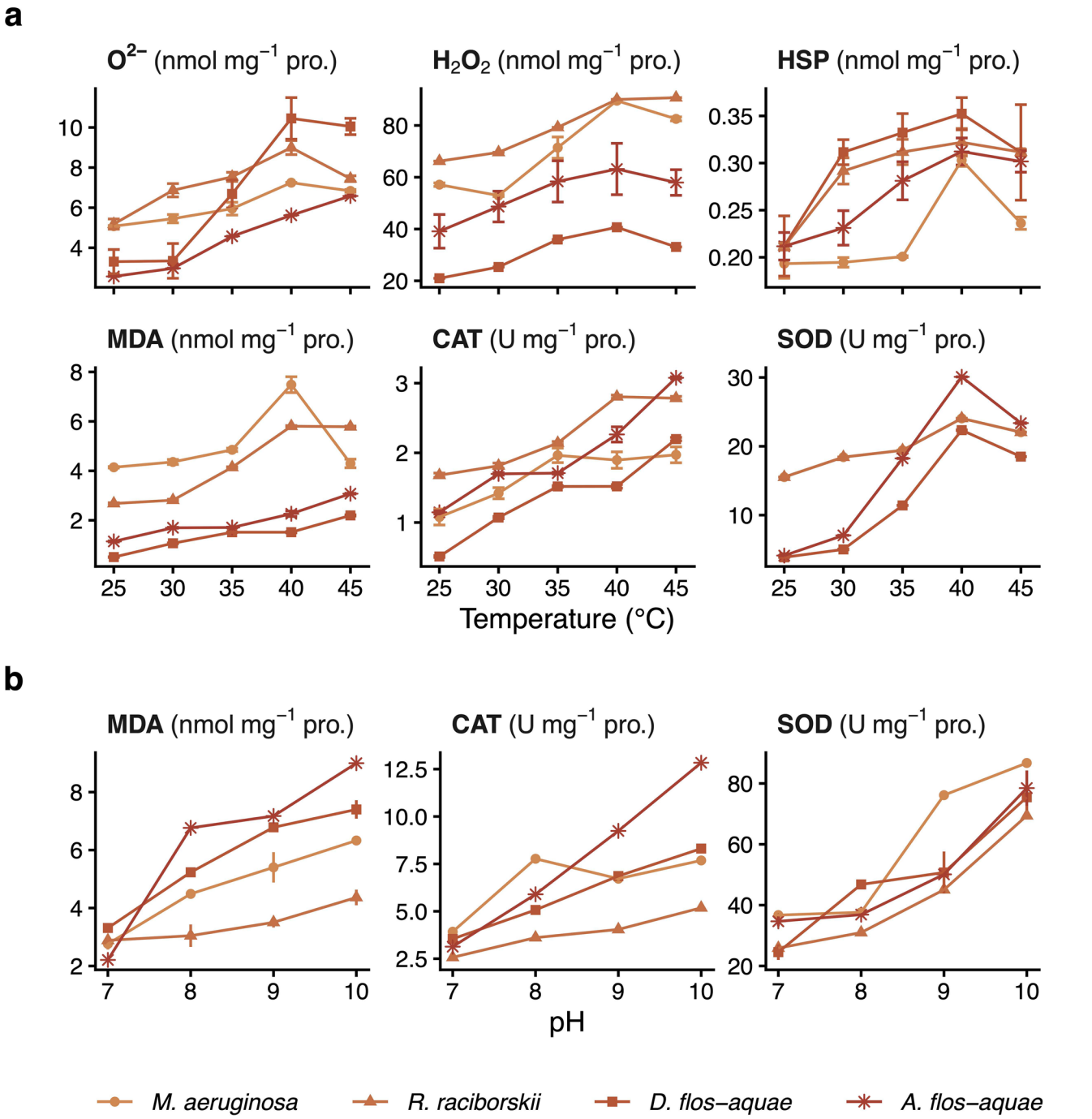

Fig. 2 | Oxidative stress responses and antioxidant defenses of harmful bloom-forming algae (HBFA) under thermal and alkaline stress. a Changes in intracellular reactive oxygen species (ROS; O_2^-, H_2O_2), superoxide dismutase (SOD) activity, malondialdehyde (MDA) content, catalase (CAT) activity, and heat shock proteins rose (HSP) abundance in *Microcystis aeruginosa*, *Raphidiopsis raciborskii*, *Dolichospermum flos-aquae*, and *Aphanizomenon flos-aquae* exposed to increasing temperatures (25–45 °C). **b** Responses of antioxidant enzyme activities (SOD and CAT) and lipid peroxidation (MDA) in the same species across an alkaline gradient (pH 7–10). Data are presented as mean ± SD ($n = 5$). $n = 5$ refers to biological replicates, i.e., five independent culture flasks per treatment for each species. All biochemical parameters were normalized to protein content.

obliquus and *Chlorella* under heat stress[23], and demonstrate that HBFA engage heat-stress priming mechanisms that contribute to the establishment of thermal memory[24]. The transient fall in F_v/F_m is consistent with accelerated PSII damage and impaired D1 repair[25]. However, cell density still increased at 40 °C, suggesting activation of heat-resilient metabolic pathways, including heterotrophic carbon use and nutrient remobilization[26].

Recovery assays showed that photosynthetic performance and growth were rapidly restored when the temperature returned to 25 °C (Fig. S2b), demonstrating pronounced thermal plasticity. This response parallels findings in *Pyropia yezoensis*, where non-lethal heat priming establishes heat-stress memory and improves post-stress survival[27]. The enhanced tolerance in this red alga is partly attributed to memory-driven induction of nutrient transporter genes, which promotes nutrient acquisition and post-stress growth[28]. Consistent with these priming phenomena, HBFA in our study exhibited marked increases in cellular protectants: heat shock proteins rose (HSP) by 47.5–66.2% and polyP by 57.9–197.0% at 40 °C relative to 25 °C

(Figs. 2a and 3a). Although HSP stabilize protein complexes during thermal stress, polyP provides the central metabolic and redox buffering capacity that underpins sustained heat tolerance[29]. Acting as a dynamic energy reservoir, polyP supports ATP regeneration and antioxidant defenses[30], and helps maintain ATP/ADP balance under fluctuating thermal conditions[31]. Heatwaves also promoted nutrient acquisition, as intracellular TP and dissolved inorganic phosphorus (DIP) increased by 18.4–86.5% and 36.7–93.1%, respectively, at 40 °C (Fig. 3b), consistent with heat-induced luxury phosphorus uptake through high-affinity transport systems[32]. Together, these responses indicate that heatwaves prime HBFA for enhanced phosphorus acquisition and structural stabilization, enabling rapid recovery once thermal stress subsides.

Bloom intensification during heatwaves substantially enhances photosynthetic CO_2 uptake, which in turn elevates water pH, often exceeding 9 in eutrophic lakes[33]. To mechanistically resolve how HBFA withstand such thermo-alkaline conditions, we assessed cellular responses under controlled alkaline stress. Stabilisomes, which are polyP-rich, high-density granules that function both as intracellular phosphorus reservoirs and as biomechanical ballast structures, were examined as a potential mediator of resilience. Exposure to pH 10 led to sharp increases in intracellular TP, DIP, and polyP (27.1–209.1%, 81.6–156.4%, and 98.5–153.5% relative to pH 7), together with elevated activities of SOD and CAT and higher MDA levels (Figs. 2b and 3d). These responses indicate that alkalinity stimulates luxury phosphorus uptake, providing abundant substrate for polyP synthesis and thereby strengthening intracellular phosphorus storage and metabolic robustness[34]. Consistent with this pattern, *Microcystis aeruginosa* exhibits heightened ROS production, lipid peroxidation, and antioxidant activity at high pH 9[35]. Taken together, these findings show that polyP plays dual protective roles under alkaline stress by buffering oxidative damage and maintaining intracellular phosphate homeostasis, thereby stabilizing cellular metabolism[36,37]. PolyP accumulation therefore emerges as a central mechanism enabling HBFA to preserve metabolic integrity and withstand oxidative pressure in alkaline environments.

The alkaline responses observed in HBFA are mirrored across diverse bloom-forming taxa and natural systems, indicating that thermo-alkaline coupling is broadly conserved. In *Aphanizomenon flos-aquae*, elevated pH (pH 8) activates alkaline phosphatase (APase), enabling the mobilization of organic phosphorus that sustains growth under external phosphorus limitation[38]. Cyanobacterial mats show a similar response, in which high APase activity is coupled with coordinated polyP accumulation to maintain growth during fluctuating phosphate availability[39,40]. Field observations from Lake Taihu further support this coupling: during bloom seasons, increases in water temperature (26–35 °C), pH (8.6–9.2), and intracellular phosphorus content occurred simultaneously (Fig. S3c), indicating that thermo-alkaline stress is closely linked to enhanced phosphorus assimilation. Comparable alkalinization has been reported across diverse lake systems, including Lake Erie (*Microcystis*; pH > 9.5, episodically ~11), Upper Klamath Lake (*Aphanizomenon*; pH > 9), and Lake Bogoria (*Arthrospira*; ~10.5)[41,42]. Collectively, these patterns suggest that elevated pH is an intrinsic metabolic feedback of bloom development rather than an externally imposed condition.

Having established the ubiquity of thermo-alkaline coupling, we next asked whether these responses exhibit persistence or priming effects. PolyP continued to accumulate even after temperature had stabilized (Fig. S3d), and algae pre-exposed to pH 10 recovered more rapidly than those pre-conditioned at pH 8 (Fig. S2c). These patterns indicate that alkaline pre-conditioning can establish a primed state analogous to thermal acclimation. They also support the view that heatwaves and elevated pH interact to initiate a cascade of polyP-mediated stress responses in HBFA. By simultaneously enhancing phosphorus retention and oxidative stress tolerance, these responses generate a thermo-alkaline amplification effect that reinforces HBFA persistence. The resulting positive feedback loop strengthens bloom resilience and may accelerate eutrophication under increasingly frequent climate extremes.

While polyP accumulation under thermo-alkaline stress enhances metabolic stability, bloom persistence requires additional ecological strategies (e.g., buoyancy-driven vertical migration) that translate intracellular resilience into improved opportunities for nutrient acquisition and stress avoidance. *Microcystis* and other buoyant taxa modulate intracellular carbohydrate ballast and gas vesicles to adjust buoyancy and descend under adverse conditions[32,43], a metabolically regulated avoidance behavior that promotes bloom stability and expansion[44]. Rising temperatures further accelerate buoyancy regulation and vertical migration in *Microcystis*, facilitating rapid redistribution within the water column[45]. Beyond providing temporary refuge from photoinhibition and oxidative damage, this vertical repositioning enables access to sediment-derived phosphorus, thereby reinforcing bloom persistence.

In the context of these thermo-alkaline and nutrient-mediated responses, our results identify stabilisome formation as an additional and critical pathway underpinning HBFA resilience. Microscopy revealed that stabilisomes are ubiquitous among bloom-forming aglae and accumulate prominently in actively growing cells exposed to either 40 °C or pH 10, conditions under which cell density and downward migration were consistently enhanced (Figs. 3 and 4). Functionally, stabilisomes act as high-density intracellular ballasts that promote sinking, as their bulk density (1.79–3.13 g cm^{-3}) far exceeds that of major cellular constituents, including proteins (1.3–1.43 g cm^{-3}), nucleic acids (2 g cm^{-3}), carbohydrates (1.55–1.62 g cm^{-3}), and lipids (0.91–1.01 g cm^{-3})[46]. Vertical migration assays corroborated this role, showing that heat-induced stabilisome proliferation across both unicellular and filamentous HBFA resulted in substantially greater algal accumulation at depths of 15–30 cm relative to surface layers (Fig. 4a, b). Under non-stress conditions, polyP stored within stabilisomes can be rapidly mobilized as a preferential phosphorus source to support macromolecular synthesis and restore buoyancy[7], enabling reversible control of cellular density. This dynamic regulation is especially pronounced in small unicellular or colonial taxa, whereas vertical migration in larger taxa is further shaped by colony size, aggregation, and the balance between buoyancy and drag forces[43,47].

Thus, stabilisome accumulation complements the canonical carbohydrate–gas vesicle buoyancy system by providing a biomechanical means for cells to alternate between deep, stress-protected refuges and light-rich surface waters. This stress-induced, metabolically powered density cycling tightly couples nutrient acquisition with stress avoidance, positioning stabilisomes as both biochemical reserves and dynamic regulators of vertical mobility that enhance HBFA growth. By enabling rapid redistribution within the water column, this mechanism confers resilience under thermal and chemical extremes and reinforces the positive feedbacks characteristic of thermo-alkaline amplification.

Extreme precipitation increases phosphorus pulse inputs and facilitates rapid HBFA assimilation

In addition to thermo-alkaline amplification, bloom initiation and persistence depend critically on short-lived nutrient pulses generated by hydrological extremes. Intense precipitation mobilizes particle-bound phosphorus through watershed runoff and sediment disturbance, producing high-concentration inputs that can substantially supplement algal nutrition[48]. Because such events typically occur during warm seasons when sedimentary phosphorus desorption is temperature sensitive, precipitation-driven resuspension and thermal conditions often co-occur in ways that jointly influence nutrient mobilization. Laboratory assays further showed that DIP and TP released from suspended solids and sediments increased by ~1.57–9.43

https://doi.org/10.1038/s41467-026-69529-3

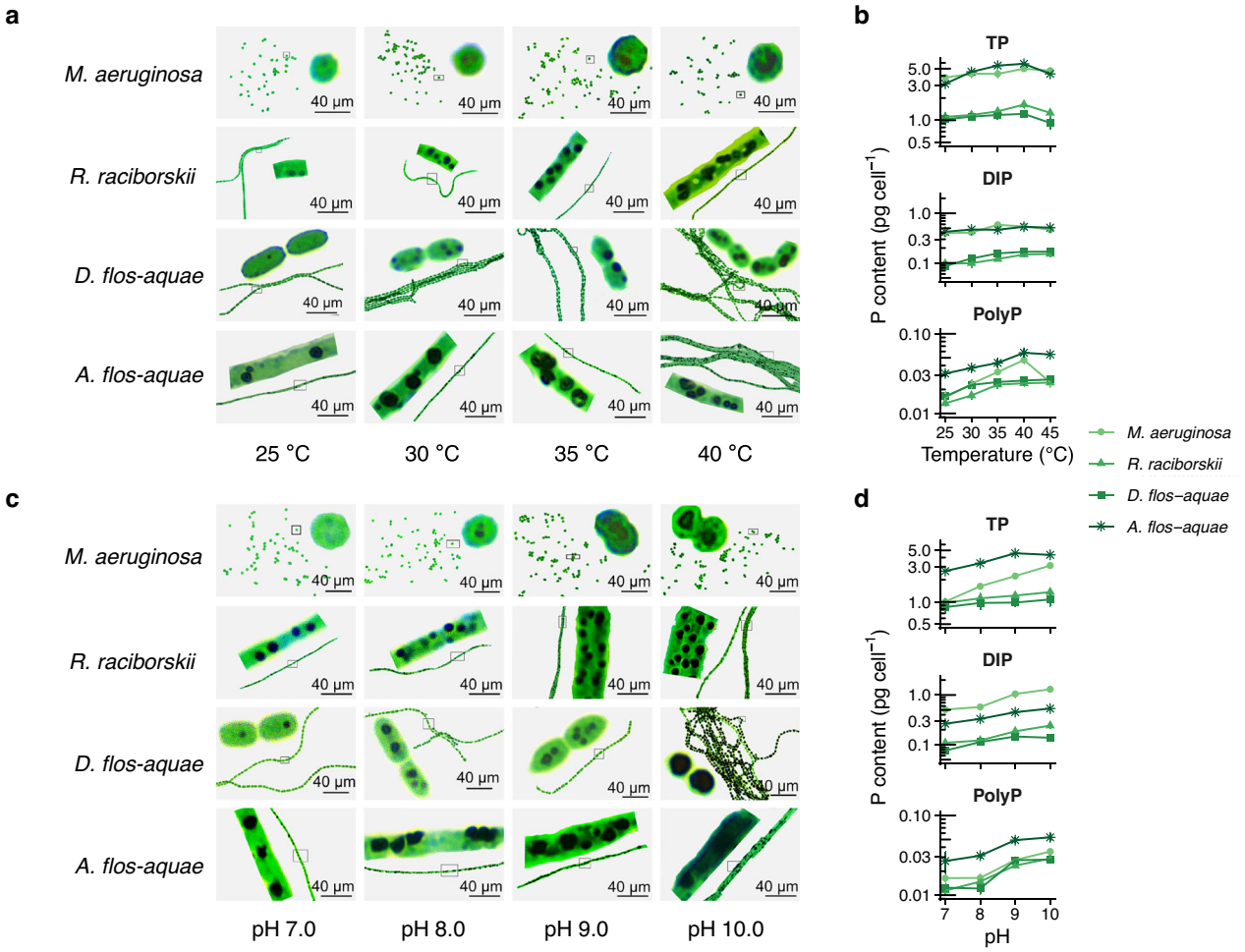

Fig. 3 | Stress-induced stabilisome formation and phosphorus reallocation in bloom-forming algae (HBFA). a Representative micrographs showing the formation of stabilisomes (polyphosphate [polyP]-rich intracellular structures) in *Microcystis aeruginosa*, *Raphidiopsis raciborskii*, *Dolichospermum flos-aquae*, and *Aphanizomenon flos-aquae* exposed to increasing temperatures (25–40 °C). Stabilisomes appear as dark-stained polyP-rich inclusions within cells. Scale bars, 40 µm. **b** Temperature-dependent changes in cellular phosphorus fractions, including total phosphorus (TP), inorganic phosphorus (DIP), and polyP, in the four species shown in (**a**). **c** Representative micrographs illustrating stabilisome formation in the same species across an alkaline gradient (pH 7.0–10.0). Scale bars, 40 µm. **d** Corresponding variations in cellular TP, DIP, and polyP contents under different pH conditions. Data are presented as mean ± SD ($n = 5$). $n = 5$ refers to biological replicates, i.e., five independent culture flasks per treatment for each species.

fold at 25–35 °C relative to 15 °C (Fig. 5b, c), indicating that precipitation-driven mixing and temperature-enhanced desorption can act synergistically to accelerate phosphorus release. Consistent with this mechanism, declines in precipitation intensity were accompanied by reduced Chl-a concentrations, reflecting diminished external nutrient delivery (Fig. S1a). Similar hydrologically induced nutrient mobilization has been reported in the North American Great Lakes, where disturbed particulate phosphorus constitutes a major source of phytoplankton nutrition[49].

Once mobilized into the water column, this storm-driven phosphorus is rapidly assimilated by HBFA. Within 4 h at elevated temperature, DIP uptake increased by 201.1–2,011.1% relative to initial cellular content, far exceeding immediate metabolic requirements, whereas TP increased by 142.2–868.0% (Fig. 5d, e). This disparity reflects classic luxury uptake, whereby excess phosphorus is sequestered intracellularly as polyP, transforming brief hydrological inputs into durable biochemical reserves[48,50]. Field and experimental evidence further indicates that storm-mobilized particulate phosphorus represents a major component of the bioavailable pool and is rapidly intercepted by algae before it can resettle[50–52]. Thus, precipitation pulses not only trigger bloom onset but also facilitate metabolic "investment" into polyP reserves that enhance resilience to subsequent stressors[7].

The ability to convert pulsed phosphorus inputs into polyP stores is not unique to HBFA but reflects a deeply conserved algal strategy. PolyP metabolism is widely conserved across algal groups and underpins resilience to diverse environmental disturbances. In cyanobacteria, polyP contributes to energy regulation and stress survival[34], whereas in *Karenia mikimotoi* and *Achnanthidium minutissimum*, both polyP content and gene expression respond sharply to external phosphorus availability[53,54]. Even picoplankton in oligotrophic systems sustain high productivity through efficient polyP accumulation and recycling[55]. This conserved strategy is mirrored during extreme precipitation, when storm-driven phosphorus surpluses are rapidly assimilated and converted into polyP, effectively extending the pulse memory of short-lived hydrological inputs. Collectively, these findings identify polyP accumulation as a universal mechanism that enables HBFA to convert transient nutrient pulses into a sustained biochemical capacity for coping with later stress.

Once formed during nutrient pulses, these polyP reserves continue to support bloom development even in the absence of new external inputs. Beyond intracellular granules, polyP is stored across

https://doi.org/10.1038/s41467-026-69529-3

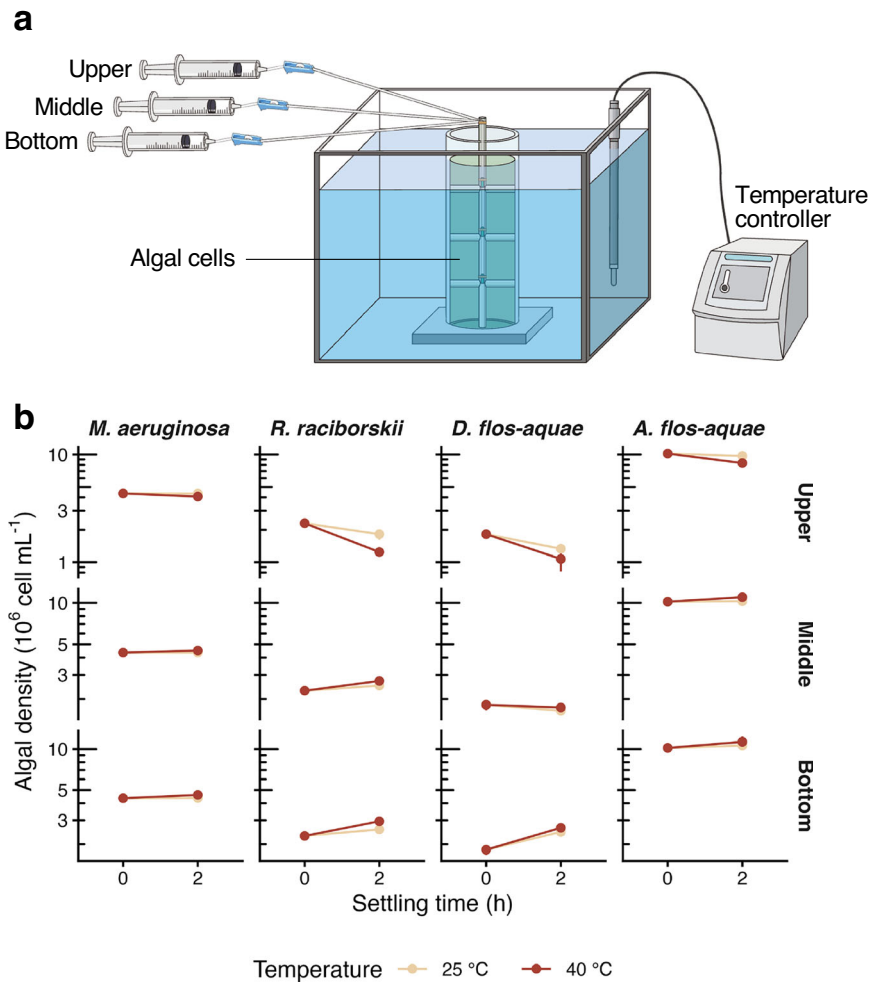

Fig. 4 | Stabilisome-associated vertical redistribution of bloom-forming algae (HBFA) under thermal stress. a Schematic diagram of the experimental column system used to examine vertical redistribution of algal cells under controlled temperature conditions. Algal suspensions were incubated in a cylindrical column placed within a temperature-controlled water bath, and samples were collected from the upper, middle, and bottom layers at designated time points. **b** Changes in algal cell density at different vertical positions (upper, middle, and bottom layers) over settling time (0–2 h) for *Microcystis aeruginosa*, *Raphidiopsis raciborskii*, *Dolichospermum flos-aquae*, and *Aphanizomenon flos-aquae* under 25 °C and 40 °C conditions. Data are means of biological replicates ($n = 5$ independent experimental columns per treatment; experimental unit = column).

multiple ecological compartments, including cyanobacterial mats, sediment–water interface layers, and the extracellular polymeric substances of large colonies, forming a distributed internal phosphorus reservoir that buffers cells against fluctuations in external supply. Cyanobacterial mats, for example, rapidly accumulate polyP and maintain stoichiometric flexibility under shifting phosphate regimes[42], while biogenic polyP in sediments contributes to seasonal phosphorus release that remains bioavailable during subsequent stratification or resuspension events[56]. These internal-storage pathways help explain why load-reduction programs often yield delayed or muted improvements in water quality, because internal polyP pools can continue to support biomass persistence even as external inputs decline[57]. Extreme precipitation further reinforces this internal reservoir by mobilizing particle-bound phosphorus that is rapidly intercepted and incorporated into polyP before resettling, effectively renewing the internal pool on each hydrological cycle. Consequently, polyP acts not only as a biochemical reserve that stabilizes HBFA under heat and alkaline stress, but also as a mechanism that converts episodic hydrological disturbances into long-lived metabolic reinforcement.

This reservoir function of polyP is not limited to eutrophic systems. In oligotrophic lakes, even modest precipitation-induced increases in phosphorus can reach thresholds sufficient for HBFA uptake. Under such transient enrichment, HBFA activate APase and mobilize organic phosphorus to meet their nutritional demand[58]. PolyP pathways frequently operate in parallel with these enzymatic mechanisms, providing dual safeguards against nutrient fluctuation[37,59]. Consequently, luxury phosphorus uptake and polyP storage confer adaptive advantages in both eutrophic and nutrient-poor systems. Despite this broad functional role, further work is needed to resolve how thermal stress, hydrological variability, and cellular physiological adjustments interact to support bloom persistence and intensification under extreme climatic conditions.

A unified framework linking climate extremes to bloom persistence

Our findings demonstrate that short-lived, high-intensity climate extremes exert disproportionate control over the intensification and persistence of HBFA. To integrate these processes, we propose a unified conceptual framework (Fig. S5), the thermo-alkaline cascade amplification model, in which cellular and ecological adjustments enable HBFA to convert episodic environmental shocks into sustained ecological advantage. Heatwaves impose strong oxidative stress that activates antioxidant defenses, stimulates phosphorus uptake, and drives substantial polyP accumulation. In parallel, HBFA deploys a

https://doi.org/10.1038/s41467-026-69529-3

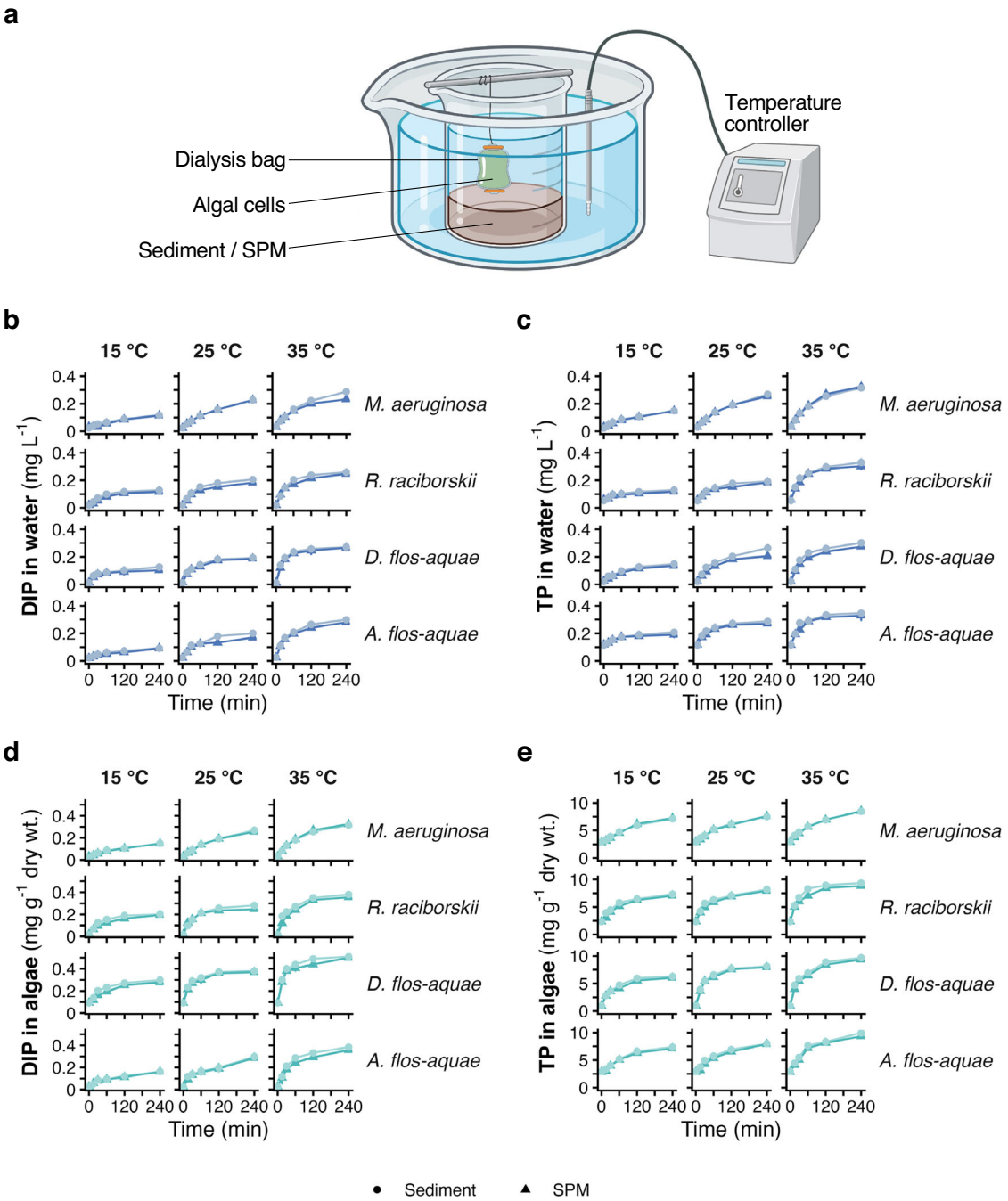

Fig. 5 | Temperature-induced phosphorus fluxes from sediments and suspended particles. a Schematic diagram of the experimental system used to quantify phosphorus fluxes between sediment or suspended particulate matter (SPM) and algal cells under controlled temperature conditions. Algal cells were enclosed in dialysis bags and incubated in contact with sediment or SPM, allowing molecular exchange without direct physical contact between cells and particles, within a temperature-controlled water bath. Temporal changes in inorganic phosphorus (DIP) (**b**) and total phosphorus (TP) (**c**) concentrations in the surrounding water over time (0–240 min) at 15, 25, and 35 °C for *Microcystis aeruginosa*, *Raphidiopsis raciborskii*, *Dolichospermum flos-aquae*, and *Aphanizomenon flos-aquae*. Corresponding accumulation of intracellular DIP (**d**) and TP (**e**) in algae under the same temperature treatments, expressed on a dry weight basis.

stabilisome-based ballast system that facilitates downward migration into cooler, deeper waters where cells can continue proliferating using previously stored luxury phosphorus. As bloom biomass increases, photosynthetic CO_2 drawdown elevates water pH, initiating a secondary alkaline loop that further enhances buoyancy regulation and intracellular polyP storage. Together, these responses recast heatwaves and elevated pH not simply as stressors but as ecological cues that activate resource-conserving strategies, positioning stress resistance as a central mechanism linking climate extremes to bloom persistence.

Extreme precipitation further strengthens this cascade by rapidly increasing the pool of bioavailable phosphorus for immediate assimilation. The resulting pulses enhance polyP storage, antioxidant capacity, and metabolic flexibility, providing resilience during subsequent thermal stress. Consistent with these patterns, incorporating precipitation into temperature-based GAMs increased the explanatory strength of temperature effects on Chl-a across both trophic states. Specifically, the deviance explained by temperature increased from 0.138 to 0.153 in oligotrophic lakes and from 0.093 to 0.146 in eutrophic lakes when precipitation was included

https://doi.org/10.1038/s41467-026-69529-3

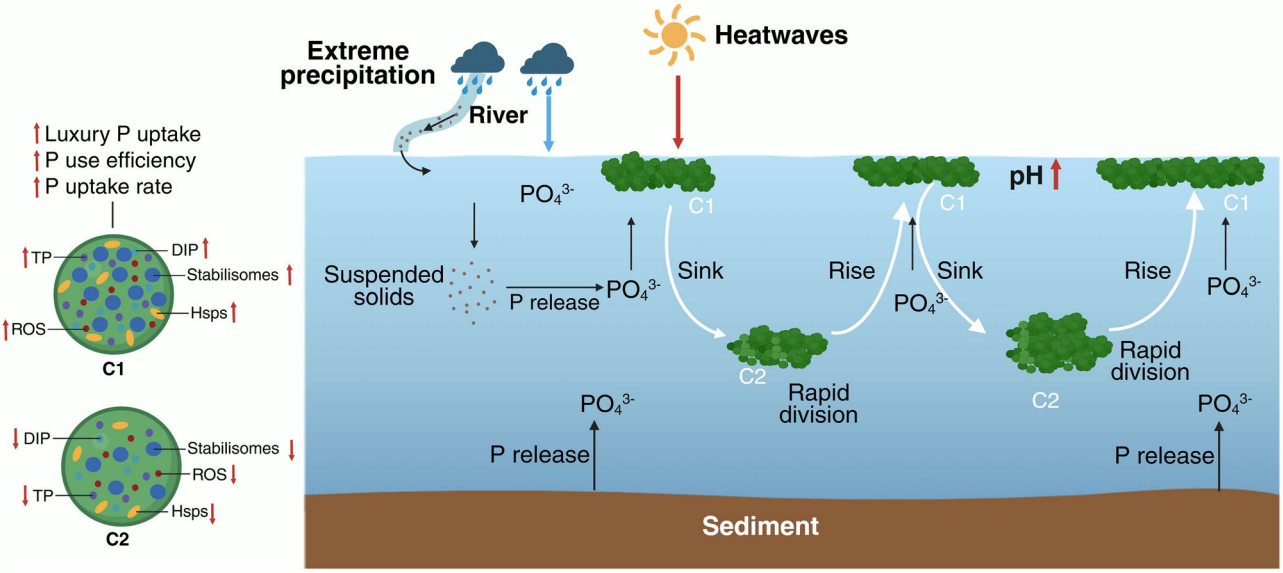

Fig. 6 | Conceptual model linking climate extremes to bloom persistence through thermo-alkaline amplification and nutrient-pulse assimilation. Heatwaves induce oxidative stress in bloom-forming algae (HBFA), triggering rapid polyphosphate (polyP) accumulation and stabilisome formation. These high-density intracellular structures increase cellular ballast and promote downward migration, enabling HBFA to temporarily evade thermal stress while accessing sediment-associated phosphorus. As bloom biomass accumulates, enhanced photosynthetic CO_2 drawdown elevates water pH, activating a secondary alkaline feedback that further promotes polyP storage and buoyancy regulation. Extreme precipitation events mobilize suspended-solid- and sediment-bound phosphorus, generating short-lived but intense nutrient pulses that are rapidly assimilated and stored as intracellular polyP. When precipitation-driven phosphorus pulses occur in temporal sequence with heatwaves, polyP accumulation, stabilisome-mediated vertical redistribution, and bloom expansion are synergistically amplified. Together, these coupled thermo-alkaline and hydrological processes form a climate-extreme-driven feedback loop that converts episodic environmental shocks into sustained nutrient access, enhanced stress tolerance, and prolonged bloom persistence.

(Fig. S4a–d), indicating that precipitation enhances temperature-driven Chl-a variability rather than acting as an independent driver. When storm-driven phosphorus pulses recur in sequence with heatwaves, their effects compound, as phosphorus accumulated during precipitation events becomes a critical internal reserve during later heat stress, supporting continued proliferation and enabling vertical redistribution. This climate-rhythm coupling sustains bloom persistence even in oligotrophic lakes, illustrating how HBFA convert episodic environmental shocks into long-lived ecological advantage.

Collectively, our results show that episodic climate extremes mobilize nutrient pulses, accelerate their biological capture, and initiate self-reinforcing feedback loops that enhance algal resilience far more rapidly than gradual climate trends. When anthropogenic influences are removed, temperature anomalies and precipitation extremes exert particularly strong control over lake Chl-a variability, highlighting the acute sensitivity of bloom trajectories to short-term climatic perturbations. Heatwaves induce oxidative stress that stimulates polyP accumulation and antioxidant activation, while bloom-driven CO_2 depletion elevates pH, forming a thermo-alkaline amplification cycle in which stabilisome accumulation accelerates downward migration and deep-water refuge. Extreme precipitation, by contrast, mobilizes sediment- and particle-bound phosphorus that is rapidly assimilated before resettling, and when such pulses coincide with heatwaves, nutrient-retention and thermal-priming mechanisms act jointly to expand blooms beyond what either stressor could induce alone (Fig. 6). These integrated mechanisms explain how climate extremes intensify global eutrophication by enabling HBFA to convert transient shocks into sustained biomass advantage. As climate extremes become more frequent, bloom trajectories will increasingly be governed by the timing, intensity, and co-occurrence of heatwaves and hydrological pulses rather than by gradual warming or mean precipitation alone.

Methods

Data sources

In this study, global lake algal bloom dynamics were characterized using a recently published global lake algal bloom dataset developed by Wang et al.[60] (https://doi.org/10.1093/nsr/nwaf011). The dataset is derived from the complete MODIS–Aqua archive spanning 2003–2022 and comprises ~0.8 million satellite images with a temporal resolution of 1–2 days. It covers 1956 large freshwater lakes with surface areas greater than 50 km^2, representing ~51% of the global freshwater lake area. For the GAM analyses, we further focused on algal bloom frequency in 607 large shallow lakes worldwide that experienced persistent blooms for more than 10 years during 2003–2022.

Algal bloom detection is based on Rayleigh-corrected reflectance (Rrc) and a normalized Floating Algal Index (nFAI), which is specifically optimized for detecting surface and near-surface algal accumulations. To reduce non-algal interference, CIE color space masking was applied to distinguish algal blooms from suspended sediments, and floating-leaved macrophytes were excluded using the Global Surface Water Occurrence dataset. This multi-step processing framework effectively minimizes misclassification arising from atmospheric correction errors, cloud contamination, sun glint, and shoreline mixed-pixel effects.

The bloom detection algorithm has been systematically validated across lakes from multiple climatic and geographic regions using independent visual interpretation and in situ observations, achieving an overall classification accuracy of ~81%. Moreover, the dataset is constructed from a single, internally consistent sensor (MODIS–Aqua), thereby avoiding cross-sensor inconsistencies and temporal discontinuities that may affect multi-sensor merged Chl-a products.

In this study, annual algal bloom frequency at the lake scale was defined as the ratio of bloom-positive observations to the total number of valid satellite observations within a given year. Lake-level bloom frequency metrics were subsequently aggregated to the global scale

and integrated with climate extreme indices and socioeconomic variables for subsequent statistical analyses.

To complement the satellite observations and provide partial ground-truthing, we also incorporated a long-term in situ dataset comprising 547 lakes worldwide, originally compiled by Qin et al.[61]. Although widely used for ecological assessments, this dataset has not previously been examined in the context of population density, temperature, or precipitation. The integration of satellite and in situ records, therefore, provides a more robust and representative basis for assessing global eutrophication dynamics and their climatic and demographic drivers.

Annual anomalies in global land temperature (2003–2022), global surface air temperature increases relative to the 1850–1900 pre-industrial baseline, and global daily precipitation were obtained from the ERA5 reanalysis dataset produced by the European Center for Medium-Range Weather Forecasts and routinely disseminated through the Copernicus Climate Change Service. These datasets enabled the large-scale analysis of temperature- and precipitation-driven variation in algal bloom dynamics. From the daily precipitation fields, we computed three widely used indices of extreme rainfall: Rx1day, the annual maximum 1-day precipitation amount; R95p, the annual total precipitation from days exceeding the 95th percentile of the reference period; and PTOT, the cumulative precipitation associated with extreme events above the 95th percentile, which serves as a proxy for cumulative intense rainfall[62]. Global human population data were obtained from the United Nations World Population Prospects (https://population.un.org/wpp/). Lake-specific population density was derived from the WorldPop global population dataset (https://www.worldpop.org/) in combination with the GeoNames geographical database (http://www.geonames.org/), providing spatially explicit demographic information for watershed-scale analyses.

Preparation of HBFA and measurement of HBFA stress responses

The resistance mechanisms of HBFA under climate extremes were investigated using *M. aeruginosa*, *Raphidiopsis raciborskii*, *Dolichospermum flos-aquae*, *Aphanizomenon flos-aquae*, all of which are globally dominant harmful bloom-forming algae. Cultures were obtained from the Institute of Aquatic Biology, Chinese Academy of Sciences, and maintained in BG11 medium at 25 °C under a 12 h light/12 h dark photoperiod with a light intensity of 33 μmol photons $m^{-2} s^{-1}$. Cells were agitated three times daily and harvested during exponential growth by centrifugation (~1790 × *g*, 10 min). The pellet was resuspended in 2 L of BG11 medium, homogenized, and evenly distributed into fifteen 250-mL Erlenmeyer flasks. For temperature treatments, cultures were incubated at 25, 30, 35, 40, and 45 °C at a constant pH of 7. For pH treatments, cultures were maintained at 25 °C and adjusted to pH 7, 8, 9, or 10 using dilute HCl or NaOH prepared in BG11. All incubations were performed under a 12 h light/12 h dark cycle (33 μmol photons $m^{-2} s^{-1}$) with shaking at 150 rpm for 4 h per day to ensure culture homogeneity.

At the end of each experiment, all four HBFA species were analyzed for a suite of physiological and biochemical parameters, including phosphorus fractions, superoxide anion and hydrogen peroxide levels, antioxidant enzyme activities, heat shock protein abundance, photosynthetic performance, cell density, and activities of growth-related enzymes. To evaluate recovery from heat stress, cultures exposed to 35 °C and 40 °C were subsequently transferred to 25 °C and maintained for an additional 4 days under the same conditions as the 25 °C control. Likewise, after 4 h of alkaline exposure at pH 9 or 10, cultures were adjusted to pH 8 and incubated for 4 days under the conditions used for the pH 8 control. MDA content, SOD and CAT activities, Chl-a concentration, and cell density were quantified on Days 1 and 4 of the recovery phase.

To assess whether stabilisomes are present in natural HBFA populations, in situ bloom samples were collected during active bloom events from Lake Chaohu, Lake Hulun, Lake Tianlai, Lake Dianchi, Lake Taihu, and Lake Khanka (Fig. S3a, b, Table S1). Stabilisomes in all HBFA samples were visualized using a modified Albert staining procedure following the manufacturer's protocol (Cat. RS4253, Lot 20250917, G-CLONE, Beijing, China).

Stabilisome-mediated vertical migration was examined using axenic cultures of *A. flos-aquae*, *D. flos-aquae*, *R. raciborskii*, and *M. aeruginosa*. Before the vertical migration assays, cultures were ultrasonicated for 1 min at 60% amplitude to disperse filaments into single trichomes and to break *Microcystis* colonies into unicells; dispersion was confirmed microscopically. Initial cell densities were standardized to 2.0×10^6, 2.4×10^6, 2.3×10^6, and 2.5×10^6 cells mL^{-1} for the four strains, respectively. Algal suspensions were transferred into cylindrical glass columns (10 cm diameter) wrapped in black paper to eliminate lateral illumination. Each column was fitted with a central vertical rod (0.8 cm diameter) holding three silicone sampling ports (3 mm diameter) positioned at depths of 2, 15, and 30 cm. The ports remained clamped until sampling to prevent unintended exchange. Columns were then incubated at either 25 °C or 40 °C for 1 h ($n = 5$ biological replicates per treatment). Following incubation, 5-mL subsamples were gently withdrawn from each depth using sterile syringes, and algal cell densities were quantified.

Field in situ simulation experiment

Algal bloom material was collected from Lake Taihu using a 64-μm mesh phytoplankton net to concentrate cells on 8 September 2022. In situ water quality and ambient conditions during sampling were TP = 0.076 mg L^{-1}, TN = 1.03 mg L^{-1}, DO = 8.1 mg L^{-1}, with air temperature, light intensity, and UV radiation ranging from 26–35 °C, 0–530 μmol photons $m^{-2} s^{-1}$, and 0–45.9 μW cm^{-2}, respectively. A 20-mL aliquot of the concentrated suspension was placed between two 0.45-μm filter membranes, secured between acrylic plates, and clamped to maintain structural integrity. Six time-series groups were prepared ($n = 5$ replicates per group), and samples were harvested at 0, 4, 8, 12, 16, and 20 h. At each time point, the material was divided into four equal subsamples and transferred into 50-mL centrifuge tubes (Tubes 1–4). Tube 1 was fixed with 15 mL of formaldehyde for algal cell density determination; Tube 2 was fixed with 15 mL of trichloroacetic acid for intracellular DIP measurement; Tube 3 was treated with 15 mL of alkaline sodium hypochlorite for intracellular polyP determination; and Tube 4 was left unfixed for subsequent intracellular TP analysis. All fixed samples were stored at 4 °C in insulated containers and transported to the laboratory for chemical and microscopic analyses.

Surface sediments (0–10 cm) were collected from Lake Taihu using a Petersen grab sampler (HNM1-2), sealed immediately, kept in the dark, and transported to the laboratory, where coarse debris (e.g., branches, leaves, shell fragments) was manually removed. Suspended solids were obtained by sampling lake water 10 cm below the surface, passing it through a 200-mesh sieve to remove large particulates, and retaining the resulting suspension. Additional algal material from Lake Taihu was collected, harvested by centrifugation (50-mL tubes, ~1010 × *g*, 15 min), washed three times with phosphorus-free BG11 medium, and resuspended in 500 mL of phosphorus-free BG11 to induce phosphorus starvation. Cultures were maintained for 8 days under standardized conditions (25 °C, 41 μmol photons $m^{-2} s^{-1}$, 14 h light/10 h dark cycle, pH 8). The experiment comprised two treatment groups, sediment and suspended solids, each with three temperature regimes (15, 25, and 35 °C) and three biological replicates. For the sediment treatment, 100 mL of sediment was added to 800 mL of phosphorus-free BG11 medium, whereas for the suspended-solids treatment, 100 mL of collected particulates was added to 800 mL of medium. All flasks were equilibrated to the designated temperature.

Subsequently, 100 mL of the phosphorus-starved algal culture (1×10^8 cells mL^{-1}), enclosed in dialysis bags with a molecular weight cutoff of 100,000 Da, was introduced into each flask (Fig. 5a). During the 250-min incubation, water samples were collected every 25 min. At each time point, 8 mL of filtrate and 6 mL of algal suspension were withdrawn to quantify TP in the overlying water and in algal cells, respectively.

Measurement of water quality parameters and HBFA

Water temperature (T), dissolved oxygen (DO), and pH were measured in situ using a HACH HQ30-D multiparameter probe (Hach Corporation, Loveland, CO, USA). TP and DIP in water were quantified colorimetrically, with or without persulfate ($K_2S_2O_8$) digestion, following the protocol of Ebina et al.[63]. Intracellular TP and phosphate in algal cells were determined according to Zhou et al.[64]. Detailed step-by-step protocols for TP/DIP and intracellular TP/DIP measurements are provided in Supplementary Information. Absolute polyP was quantified by mixing 20 mL of filtered algal suspension with 2 mL of toluidine blue O (TBO) assay solution (15 mg TBO mL^{-1} in 0.1 N acetic acid) and incubating the mixture for 15 min at room temperature. A 1-mL subsample was subsequently hydrolyzed in 2 N HCl at 95 °C for 40 min, after which the released phosphate was measured using the molybdenum blue method[65]. For intracellular assays, a 3.0-mL aliquot of algal culture was centrifuged at ~16,100 × *g* for 5 min at 4 °C. The pellet was resuspended in 3.0 mL of phosphate-buffered saline (PBS, 0.05 mol L^{-1}, pH 6.8), gently mixed, and stored at −80 °C. Prior to analysis, samples underwent four freeze–thaw cycles at 25 °C to ensure complete cell lysis.

MDA content and the activities of SOD and CAT were quantified using commercial assay kits (Nanjing Jiancheng Bioengineering Institute, China; A003-1-2, A001-3-2, and A007-1-1, respectively) with absorbance read in 96-well plates. Detailed experimental procedures, calculation formulas, and quality controls are provided in Supplementary Information. Photosynthetic parameters, including Y(II), F_v/F_m, and ETR_m, were measured using a Phyto-PAM fluorometer (Heinz Walz, Germany). Chl-a was extracted with 90% acetone and quantified spectrophotometrically; the full extraction workflow and equations (Strickland and Parsons[66]) are described in Supplementary Information.

Stabilisome size and abundance were quantified by nanoparticle tracking analysis using a NanoSight NS300 (Malvern Panalytical, UK). Samples were diluted in PBS, injected into the instrument chamber, and analyzed based on Brownian motion trajectories to derive hydrodynamic diameters and particle concentrations ($n = 5$). Dry-mass concentration was determined by freeze-drying 30 mL of the extracted stabilisome suspension to constant weight and measuring the residual mass with an analytical balance. Particle density was calculated from the total dry mass, particle size, and particle number, assuming spherical geometry for individual particles ($V = 4/3\ \pi r^3$).

The influence of stabilisome accumulation on algal vertical migration was assessed using *M. aeruginosa*. Two 5-mL cultures (2×10^6 cells mL^{-1}) were exposed to either 40 °C or 25 °C for 4 h and centrifuged at their respective temperatures (~1010 × *g*, 5 min). Pellets were gently layered onto the surface of vertically oriented glass columns (25 cm length, 4 cm diameter) filled with distilled water, and sinking time to defined depths was recorded.

Data treatment and statistical analysis

For global-scale analyses, lake Chl-a, nutrient concentrations (TN and TP), and all anthropogenic and climatic predictors were $\log_{10}$-transformed prior to visualization and modeling to ensure dimensional consistency and reduce scale-dependent bias. Statistical significance was assessed at $p < 0.05$.

Nonlinear relationships between algal bloom metrics and environmental drivers were quantified using GAMs fitted with penalized smooth functions, as detailed in the Supplementary Methods. Model diagnostics, including deviance explained, effective degrees of freedom, F statistics, *p* values, and sample size, are reported in the corresponding panels.

All statistical analyses and figure generation were performed in R (version 4.4.2; R Core Team, 2023), including GAM-based response curves, variable–response relationships, and all forms of line plots (e.g., temporal trends, gradient responses, and recovery trajectories). All GAM analyses were implemented in R using the mgcv package (v1.9-4). Solid lines represent fitted relationships or mean trends, and shaded regions denote 95% confidence intervals (Supplementary Code 1).

Data availability

The data supporting the findings of this study are available within this manuscript. The data are provided in the Supplementary Information/Source Data file. Source data are provided with this paper.

Code availability

The code used in this study is provided with this manuscript.

References

1. Paerl, H. W. & Paul, V. J. Climate change: links to global expansion of harmful cyanobacteria. *Water Res.* **46**, 1349–1363 (2012).
2. Laurion, I. et al. Heat-wave effects on oxygen, nutrients, and phytoplankton can alter global warming potential of gases emitted from a small shallow lake. *Environ. Sci. Technol.* **50**, 6267–6275 (2016).
3. Kramer, B. J. & Gobler, C. J. Simulated heat waves promote the growth but suppress the N_2 fixation rates of *Dolichospermum* spp. and cyanobacterial communities in temperate lakes. *Ecol. Indic.* **147**, 109983 (2023).
4. Paerl, H. W. & Huisman, J. Climate change: a catalyst for global expansion of harmful cyanobacterial blooms. *Environ. Microbiol. Rep.* **1**, 27–37 (2009).
5. Paerl, H. W., Hall, N. S. & Calandrino, E. S. Controlling harmful cyanobacterial blooms in a world experiencing anthropogenic and climatic-induced change. *Sci. Total Environ.* **409**, 1739–1745 (2011).
6. Soranno, P. A. et al. Abrupt changes in algal biomass of thousands of US lakes are related to climate and are more likely in low-disturbance watersheds. *Proc. Natl. Acad. Sci. USA* **122**, e2416172122 (2025).
7. Li, J. & Dittrich, M. Dynamic polyphosphate metabolism in cyanobacteria responding to phosphorus availability. *Environ. Microbiol.* **21**, 572–583 (2019).
8. Chen, C., Zheng, C. Q., Wang, M. M., Yang, S. H. & Yang, L. Y. Low concentration nitrate-nitrogen improves polyphosphate accumulation in *Microcystis*. *J. Lake Sci.* **34**, 766–776 (2022).
9. Wang, C. Y. et al. High-purity isolation of polyphosphate-rich stabilisomes defines their conserved chemical architecture in thermophilic cyanobacteria. *Plants* **15**, 499 (2026).
10. Han, Y. Y. et al. Human impacts dominate global loss of lake ecosystem resilience. *Geophys. Res. Lett.* **51**, e2024GL109298 (2024).
11. Wei, Z., Yu, Y. X. & Yi, Y. J. Prediction of future chlorophyll-a concentrations in large eutrophic shallow lakes under multiple stressors. *Earth's. Future* **13**, e2024EF005293 (2025).
12. Woolway, R. I. et al. Extreme and compound events in lakes. *Nat. Rev. Earth Environ.* **6**, 593–611 (2025).
13. Shi, W. Q. et al. Global lake phytoplankton proliferation intensifies climate warming. *Nat. Commun.* **15**, 10572 (2024).
14. Ho, J. C., Michalak, A. M. & Pahlevan, N. Widespread global increase in intense lake phytoplankton blooms since the 1980s. *Nature* **574**, 667–670 (2019).

15. Gao, L. W. et al. Spatiotemporal changes in chlorophyll-a concentration in China's lakes and its driving factors. *Environ. Sci.: Process. Impacts* **27**, 1971–1987 (2025).
16. Zhang, S. et al. Climate change promotes harmful algal blooms in China's lakes and reservoirs despite significant nutrient control efforts. *Water Res.* **277**, 123307 (2025).
17. Feng, L. et al. Harmful algal blooms in inland waters. *Nat. Rev. Earth Environ.* **5**, 631–644 (2024).
18. Duan, Z. Z., Gao, W., Cheng, G. W., Zhang, Y. & Chang, X. X. Warming surface and lake heatwaves as key drivers to harmful algal blooms: a case study of Lake Dianchi, China. *J. Hydrol.* **632**, 130971 (2024).
19. Szydlowski, D. K., Bollini, K. A., Pace, M. L. & Wilkinson, G. M. Aquatic heatwaves increase surface chlorophyll concentrations in experimental and reference lakes. *Limnol. Oceanogr. Lett.* **10**, 453–463 (2025).
20. Liao, A. R., Han, D. M., Song, X. F. & Yang, S. T. Impacts of storm events on chlorophyll-a variations and controlling factors for algal bloom in a river receiving reclaimed water. *J. Environ. Manag.* **294**, 113376 (2021).
21. Pearce, N. J. T., Lu, J., Evans, M. A., Frost, P. C. & Xenopoulos, M. A. Episodic nutrient addition affects water column nutrient processing rates in river-to-lake transitional zones. *J. Geophys. Res. Biogeosci.* **126**, e2021JG006374 (2021).
22. Happe, A. et al. Nutrient pulse scenarios drive contrasting patterns in the functional stability of freshwater phytoplankton. *Limnol. Oceanogr.* **70**, 12782 (2025).
23. Akter, S., AbdElgawad, H., Beemster, G. T. S., De Boeck, G. & Schoelynck, J. Synergistic effect of nitrate exposure and heatwaves on the growth, and metabolic activity of microalgae, *Chlamydomonas reinhardtii*, and *Pseudokirchneriella subcapitata*. *Sci. Rep.* **14**, 2764 (2024).
24. Koletti, A., Skylas, D., Dervisi, I., Roussis, A. & Flemetakis, E. Oxidative stress responses in microalgae: modern insights into an old topic. *Appl. Microbiol.* **5**, 37 (2025).
25. Allakhverdiev, S. I. et al. Heat stress: an overview of molecular responses in photosynthesis. *Photosynth. Res.* **98**, 541–550 (2008).
26. Paerl, H. W. & Otten, T. G. Duelling 'CyanoHABs': unravelling the environmental drivers controlling dominance and succession among diazotrophic and non-N_2 -fixing harmful cyanobacteria. *Environ. Microbiol.* **18**, 316–324 (2016).
27. Mikami, K. Heat stress memory is critical for tolerance to recurrent thermostress in the foliose red alga *Pyropia yezoensis*. *Phycology* **5**, 28 (2025).
28. Sato, N., Kobayashi, H. & Mikami, K. Heat stress memory differentially regulates the expression of nitrogen transporter genes in the filamentous red alga '*Bangia*' sp. ESS1. *Front. Plant Sci.* **15**, 1331496 (2024).
29. Yoo, N. G. et al. Polyphosphate stabilizes protein unfolding intermediates as soluble amyloid-like oligomers. *J. Mol. Biol.* **430**, 4195–4208 (2018).
30. Rao, N. N., Gomez-Garcia, M. R. & Kornberg, A. Inorganic polyphosphate: essential for growth and survival. *Annu. Rev. Biochem.* **78**, 605–647 (2009).
31. Sebesta, J. et al. Polyphosphate kinase deletion increases laboratory productivity in cyanobacteria. *Front. Plant Sci.* **15**, 1342496 (2024).
32. Kromkamp, J. & Walsby, A. E. A computer model of buoyancy and vertical migration in cyanobacteria. *J. Plankton Res.* **12**, 161–183 (1990).
33. Yu, T. et al. Long-term trends in acid neutralizing capacity under increasing acidic deposition: a special example of eutrophic Taihu Lake, China. *Environ. Sci. Technol.* **50**, 12660–12668 (2016).
34. Sanz-Luque, E., Bhaya, D. & Grossman, A. R. Polyphosphate: a multifunctional metabolite in cyanobacteria and algae. *Front. Plant Sci.* **11**, 938 (2020).
35. Yu, J., Zhu, H., Shutes, B. & Wang, X. Y. Salt-alkalization may potentially promote *Microcystis aeruginosa* blooms and the production of microcystin-LR. *Environ. Pollut.* **301**, 118971 (2022).
36. Bossa, R., De Cunto, M., Salbitani, G. & Carfagna, S. Phosphorous utilization in microalgae: physiological aspects and applied implications. *Plants* **13**, 2127 (2024).
37. Jentzsch, L., Grossart, H. P., Plewe, S., Schulze-Makuch, D. & Goldhammer, T. Response of cyanobacterial mats to ambient phosphate fluctuations: phosphorus cycling, polyphosphate accumulation and stoichiometric flexibility. *ISME Commun.* **3**, 6 (2023).
38. Chen, X. Y. et al. Strategies adopted by *Aphanizomenon flos-aquae* in response to phosphorus deficiency and their role on growth. *Environ. Sci. Eur.* **32**, 45 (2020).
39. Li, P., Li, W. H. & Gao, K. S. Effects of temperature, pH, and UV radiation on alkaline phosphatase activity in the terrestrial cyanobacterium *Nostoc flagelliforme*. *J. Appl. Phycol.* **25**, 1031–1038 (2013).
40. Lin, W. T., Zhang, D. D. & Luo, J. F. Distribution of alkaline phosphatase genes in cyanobacteria and the role of alkaline phosphatase on the acquisition of phosphorus from dissolved organic phosphorus for cyanobacterial growth. *J. Appl. Phycol.* **30**, 839–850 (2018).
41. Eldridge, D. B., Eldridge, S. L. C., Schenk, L. N., Tanner, D. Q. & Wood, T. M. Water-quality data from Upper Klamath and Agency Lakes, Oregon, 2009-10. U.S. Geological Survey Open-File Report 2012–1142 (2012).
42. Oduor, S. O. & Schagerl, M. Phytoplankton primary productivity in three Kenyan Rift Valley saline–alkaline lakes. *Int. Rev. Hydrobiol.* **92**, 372–385 (2007).
43. Brookes, J. D. & Ganf, G. G. Variations in the buoyancy response of *Microcystis aeruginosa* to nitrogen, phosphorus and light. *J. Plankton Res.* **23**, 1399–1411 (2001).
44. Overman, C. & Wense, S. Modeling cyanobacteria vertical migration. *Water Res.* **14**, 953 (2022).
45. Feng, G. Y., Visser, P. M., Huisman, J. & Verspagen, J. M. H. Rising temperature accelerates buoyancy regulation and vertical migration of the bloom-forming cyanobacterium *Microcystis*. *Water Res.* **286**, 124259 (2025).
46. Neurohr, G. E. & Amon, A. Relevance and regulation of cell density. *Trends Cell Biol.* **30**, 171–183 (2020).
47. Aparicio Medrano, E. et al. Coupling hydrodynamics and buoyancy regulation in *Microcystis aeruginosa* for its vertical distribution in lakes. *Ecol. Model.* **248**, 41–56 (2013).
48. Davis, T. W., Berry, D. L., Boyer, G. L. & Gobler, C. J. The effects of temperature and nutrients on the growth and dynamics of toxic and non-toxic strains of *Microcystis* during cyanobacteria blooms. *Harmful Algae* **8**, 715–725 (2009).
49. Yang, X. Y. et al. Polyphosphate phosphorus in the Great Lakes. *Limnol. Oceanogr. Lett.* **9**, 602–611 (2024).
50. Orihel, D. M. et al. Internal phosphorus loading in Canadian fresh waters: a critical review and data analysis. *Can. J. Fish. Aquat. Sci.* **74**, 2005–2029 (2017).
51. Carpenter, S. R., Benson, B. J. & Kucharik, C. J. Extreme precipitation and phosphorus loads from two agricultural watersheds. *Limnol. Oceanogr.* **63**, 1221–1233 (2018).
52. Li, Y. P. et al. Storm and floods increase the duration and extent of phosphorus limitation on algal blooms in a tributary of the Three Gorges Reservoir, China. *J. Hydrol.* **607**, 127562 (2022).
53. Jin, W. Y., Chen, X. W., Tan, J. Z., Lin, X. & Ou, L. J. Variation in intracellular polyphosphate and associated gene expression in

response to different phosphorus conditions in the dinoflagellate *Karenia mikimotoi*. *Harmful Algae* **129**, 102525 (2023).
54. Lapointe, A. et al. Characterization of polyphosphate dynamics in the widespread freshwater diatom *Achnanthidium minutissimum* under varying phosphorus supplies. *J. Phycol.* **60**, 624–638 (2024).
55. Li, J., Plouchart, D., Zastepa, A. & Dittrich, M. Picoplankton accumulate and recycle polyphosphate to support high primary productivity in coastal Lake Ontario. *Sci. Rep.* **9**, 19563 (2019).
56. Schrder, L., Schmieder, P. & Hupfer, M. Biogenic polyphosphate as relevant regulator of seasonal phosphate storage in surface sediments of stratified eutrophic lakes. *Biogeochemistry* **168**, 40 (2025).
57. Duan, Z. P. et al. Phosphorus accumulation in extracellular polymeric substances (EPS) of colony-forming cyanobacteria challenges imbalanced nutrient reduction strategies in eutrophic lakes. *Environ. Sci. Technol.* **57**, 1600–1612 (2023).
58. Ji, N. N., Li, Y., Wang, S. R., Wu, Z. H. & Li, H. Buffering effect of suspended particulate matter on phosphorus cycling during transport from rivers to lakes. *Water Res.* **216**, 118350 (2022).
59. Solovchenko, A., Plouviez, M. & Khozin-Goldberg, I. Getting grip on phosphorus: potential of microalgae as a vehicle for sustainable usage of this macronutrient. *Plants* **13**, 1834 (2024).
60. Wang, Y. et al. Global elevation of algal bloom frequency in large lakes over the past two decades. *Natl. Sci. Rev.* **12**, nwaf011 (2025).
61. Qin, B. Q. et al. Water depth underpins the relative roles and fates of nitrogen and phosphorus in lakes. *Environ. Sci. Technol.* **54**, 3191–3198 (2020).
62. Li, S., Chen, Y. N., Wei, W., Fang, G. H. & Duan, W. L. The increase in extreme precipitation and its proportion over global land. *J. Hydrol.* **628**, 130456 (2024).
63. Ebina, J., Tsutsui, T. & Shirai, T. Simultaneous determination of total nitrogen and total phosphorus in water using peroxodisulfate oxidation. *Water Res.* **17**, 1721–1726 (1983).
64. Zhou, Y. et al. The distribution of phosphorus and its transformations during batch growth of *Synechocystis*. *Water Res.* **122**, 355–362 (2017).
65. Segawa, S. et al. Probiotic-derived polyphosphate enhances the epithelial barrier function and maintains intestinal homeostasis through integrin-P38 MAPK Pathway. *PLoS ONE* **6**, e23278 (2011).
66. Strickland, J. D. H. & Parsons, T. R. *A Practical Handbook of Seawater Analysis* (Fisheries Research Board of Canada, 1972).

Acknowledgements

This work was financially supported by the National Natural Science Foundation of China (Nos. 42307172 and 41871082). We sincerely thank Professor Qiao-Guo Tan (Xiamen University) for his valuable guidance and constructive suggestions on figure design and visualization.

Author contributions

W. and M.W. contributed equally to this work. L.Y. conceptualized the study and provided overall experimental guidance. M.W. and L.Y. designed the experiments. C.W. and M.W. led experimental implementation and data collection. M.W. performed experimental implementation, data analysis, and visualization. M.J.X., L.Q., M.G.C., X.H.S., J.Y., Y.W., M.X., and L.P. assisted with experimental implementation and data collection. A.-J.M. provided guidance on figure preparation and manuscript framework, and contributed to manuscript revision and language editing. Z.Z. and X.L.S. polished the language. M.W. drafted the manuscript. C.W., M.W., A.-J.M., and L.Y. revised and edited the manuscript with improvements to logic and presentation. A.-J.M. and L.Y. provided project support. All authors read and approved the final manuscript.

Competing interests

The authors declare no competing interests.

Additional information

Supplementary information The online version contains supplementary material available at https://doi.org/10.1038/s41467-026-69529-3.

Correspondence and requests for materials should be addressed to Mengmeng Wang, Ai-Jun Miao or Liuyan Yang.

Peer review information *Nature Communications* thanks the anonymous reviewers for their contribution to the peer review of this work. A peer review file is available.